Cell Death and Differentiation (2013) 20, 1101–1115

www.nature.com/cdd

Disease-relevant proteostasis regulation of cystic fibrosis transmembrane conductance regulator

VR Villella[1], S Esposito[1], EM Bruscia[1,2], M Vicinanza[3], S Cenci[4], S Guido[5], M Pettoello-Mantovani[6], R Carnuccio[7], MA De Matteis[3], A Luini[3,8], MC Maiuri[7,9], V Raia*[,10], G Kroemer*[,9,11,12,13,14] and L Maiuri*[,1,6]

Mismanaged protein trafficking by the proteostasis network contributes to several conformational diseases, including cystic fibrosis, the most frequent lethal inherited disease in Caucasians. Proteostasis regulators, as cystamine, enable the beneficial action of cystic fibrosis transmembrane conductance regulator (CFTR) potentiators in ΔF508-CFTR airways beyond drug washout. Here we tested the hypothesis that functional CFTR protein can sustain its own plasma membrane (PM) stability. Depletion or inhibition of wild-type CFTR present in bronchial epithelial cells reduced the availability of the small GTPase Rab5 by causing Rab5 sequestration within the detergent-insoluble protein fraction together with its accumulation in aggresomes. CFTR depletion decreased the recruitment of the Rab5 effector early endosome antigen 1 to endosomes, thus reducing the local generation of phosphatidylinositol-3-phosphate. This diverts recycling of surface proteins, including transferrin receptor and CFTR itself. Inhibiting CFTR function also resulted in its ubiquitination and interaction with SQSTM1/p62 at the PM, favoring its disposal. Addition of cystamine prevented the recycling defect of CFTR by enhancing BECN1 expression and reducing SQSTM1 accumulation. Our results unravel an unexpected link between CFTR protein and function, the latter regulating the levels of CFTR surface expression in a positive feed-forward loop, and highlight CFTR as a pivot of proteostasis in bronchial epithelial cells.
Cell Death and Differentiation (2013) **20,** 1101–1115; doi:10.1038/cdd.2013.46; published online 17 May 2013

Manipulating proteostasis by proteostasis regulators (PRs) has emerged as a novel therapeutic approach for the treatment of conformational diseases.[1–5] Cystic fibrosis (CF) constitutes the quintessential example of a conformational disease.[6–8] CF is a monogenic disease in which defective function of one single protein, cystic fibrosis transmembrane conductance regulator (CFTR), leads to major clinical manifestations, including chronic lung inflammation with increased susceptibility to respiratory bacterial infections, pancreatic dysfunction, raised electrolyte levels in sweat and male infertility.[9–11] CF is caused by loss-of-function mutations of CFTR, a cAMP-regulated chloride channel that is primarily located at the apical membrane of epithelial cells.[12,13] A single deletion, F508del, occurs in about 70–90% of CF patients in Northern Europe and North America.[14] Due to its misfold, ΔF508-CFTR is prematurely degraded and loses its essential ion channel activity at the plasma membrane (PM).[9,15] ΔF508-CFTR can retain channel activity if rescued at the PM by molecules that correct its intracellular retention and degradation (correctors),[16–20] as well as by low temperature,[21] but in this case ΔF508-CFTR is rapidly dismissed from the PM and redirected from endosomal recycling towards lysosomal degradation.[22,23]

We previously reported that defective CFTR function induces reactive oxygen species (ROS)-dependent and transglutaminase-2 (TGM2)-mediated sequestration of BECN1, leading to defective autophagy and increased lung inflammation.[24] PRs such as cystamine or the superoxide dismutase/catalase-mimetic EUK-134[25,26] enable the beneficial action of CFTR potentiators on ΔF508-CFTR mutant tissues well beyond drug washout through restoring BECN1 expression and autophagy, thereby reducing the abundance of SQSTM1/p62 (SQSTM1).[24,27] This might suggest that, once peripheral proteostasis has been re-established, PM-resident ΔF508-CFTR could sustain its own PM stability.

[1]Division of Genetics and Cell Biology, San Raffaele Scientific Institute, European Institute for Research in Cystic Fibrosis, Milan 20132, Italy; [2]Department of Pediatrics, Yale University School of Medicine, New Haven, CT 06509, USA; [3]Telethon Institute of Genetic and Medicine (TIGEM), Naples 80131, Italy; [4]Division of Genetics and Cell Biology, San Raffaele Scientific Institute, Milan 20132, Italy; [5]Faculty of Engineering, Federico II University, Naples 80125, Italy; [6]Institute of Pediatrics, University of Foggia, Foggia 71100, Italy; [7]Department of Experimental Pharmacology, School of Biotechnological Sciences, Federico II University, Naples 80131, Italy; [8]Institute of Protein Biochemistry, National Research Council, Naples 80131, Italy; [9]INSERM, U848, Villejuif, France; [10]Cystic Fibrosis Unit, Department of Pediatrics, Federico II University, Naples 80131, Italy; [11]Université Paris Descartes, Paris, France; [12]Metabolomics Platform, Institut Gustave Roussy, Villejuif, France; [13]Equipe 11 labellisée Ligue contre le Cancer, Centre de Recherche des Cordeliers, Paris, France and [14]Pôle de Biologie, Hôpital Européen Georges Pompidou, AP-HP, Paris, France
*Corresponding author: L Maiuri , European Institute for Research in Cystic Fibrosis, San Raffaele Scientific Institute, Division of Genetics and Cell Biology, via Olgettina 58, Milan 20132, Italy. Tel: +39 02 26434301; Fax: +39 02 26434328; E-mail: maiuri@unina.it
or V Raia, Cystic Fibrosis Unit, Department of Pediatrics, Federico II University, via S. Pansini 5, 80131, Naples, Italy. Tel: +39 081 746 3273; Fax: +39 081 746 3273; E-mail: raia@unina.it
or G Kroemer, INSERM U848, Institut Gustave Roussi, Pavillon de Recherche 1, F-94805 Villejuif, France. Tel: +33 1 42116046 ; Fax: +33 1 42116047; E-mail: kroemer@orange.fr
Keywords: CFTR; conformational diseases; protein trafficking; proteostasis; SQSTM1
Abbreviations: CF, cystic fibrosis; CFTR, cystic fibrosis transmembrane conductance regulator; PRs, proteostasis regulators; TGM2, transglutaminase-2; ROS, reactive oxygen species; PtdIns3K, type III phosphatidylinositol 3-kinase; PtdIns3*P*, phosphatidylinositol 3-phosphate; EEA-1, early endosome antigen 1; TfR, transferrin receptor; PM, plasma membrane; EGFR, epidermal growth factor receptor; Vps, vacuolar protein sorting; 3-MA, 3-methyl-adenine; LE, late endosome; PNS, post-nuclear supernatant; MTT, 3-[4,5-dimethylthiazol-2-yl]-2,5 diphenyl tetrazolium bromide; UVRAG, UV-irradiation-resistance-associated gene; CHX, cycloheximide
Received 22.11.12; revised 09.4.13; accepted 10.4.13; Edited by E Baehrecke; published online 17.5.13

Based on these premises and incognita, we explored the hypothesis that a functional CFTR might orchestrate peripheral proteostasis and ultimately regulate its own PM residence and function.

Results

CFTR depletion reduces the availability of Rab5 and impairs the recruitment of Rab5 effectors to early endosomes (EEs). The abundance of the PM pool of surface proteins/receptors that are internalized into endocytic vesicles is determined by the balance between the rate of internalization and the formation and budding of recycling tubules at EEs, where the accuracy of receptor sorting is mediated by the small GTPase Rab5 and its effectors early endosome antigen 1 (EEA-1), type III phosphatidylinositol 3-kinase (PtdIns3K, also known as hVps34, a protein that belongs to the BECN1 interactome) and its product phosphatidylinositol 3-phosphate (PtdIns3*P*).[28–31] Besides their effects on autophagy, PtdIns3K and its product PtdIns3*P* regulate endosomal fusion/maturation and trafficking.[32–34] In addition, Rab5 participates to autophagosome formation through activating hVps34, as part of the BECN1 macromolecular complex.[31]

We have reported that defective CFTR leads to functional sequestration of BECN1 interactors, including hVps34, as the result of TG2-mediated BECN1 crosslinking.[24] Therefore, we examined whether depleting CFTR from 16HBE14o- bronchial epithelial cells would also affect endocytic function.

In control conditions (i.e. 16HBE14o- cells transfected with scrambled siRNAs) the endosomal abundance of PtdIns3*P*, which can be detected with a GFP-FYVE fusion protein,[35–38] was strongly reduced after CFTR depletion (Figure 1a and Supplementary Figures S1A and B). The TGM2 inhibitor cystamine restored the endosomal localization of PtdIns3*P* to the normal level unless it was combined with the PtdIns3K inhibitor 3-methyl-adenine (3-MA) (Figure 1a).

CFTR depletion from 16HBE14o- cells lowered the cellular levels of Rab5 protein (Figure 1b). Simultaneous treatment with cystamine or transfection with HA-tagged *BECN1* (HA-*BECN1*)[24,27] abolished the reduction of Rab5 protein levels induced by CFTR depletion (Figure 1b). Depletion of *BECN1*, *VPS34* (vacuolar protein sorting 34) or *VPS15* (but not that of the autophagy-related gene product *ATG14*)[39,40] abrogated the capacity of cystamine to restore Rab5 expression (Figure 1c; Supplementary Figure S1C), indicating that these cystamine effects required a functional BECN1/hVps34/hVps15 complex.

We previously reported that defective CFTR leads to accumulation of the BECN1 interactome in the detergent-insoluble protein fraction and its sequestration within intracellular aggregates as the result of autophagy inhibition with accumulation of SQSTM1 and proteasome overload.[24] Here we show that CFTR depletion from 16HBE14o- cells resulted in the accumulation of Rab5 in the detergent-insoluble protein fraction, a phenomenon that was enhanced by the incubation with the proteasomal inhibitor MG132 (Figure 2a; Supplementary Figures S2A and B). Moreover, CFTR depletion resulted in Rab5 sequestration within HDAC6+ aggresomes (Figure 2b). These features were reversed by transfection with HA-*BECN1* or addition of cystamine unless the latter treatment was combined with hVps34 depletion (Figure 2a). Similarly to Rab5, Rab7 protein levels were significantly decreased in CFTR-depleted 16HBE14o- cells (Figure 1b) and were restored by transfection with HA-*BECN1* or cystamine, unless *BECN1*, *VPS34* or *VPS15* (but not *ATG14*) were depleted by siRNAs (Figure 1c). However, in contrast to Rab5, Rab7 did not redistribute into the insoluble protein fraction, following CFTR depletion (Figure 2a; Supplementary Figure S2B), suggesting subtle differences in the mechanisms causing the inactivation of Rab5 and Rab7.

The expression of SQSTM1 is well known to increase in conditions of autophagy impairment, because this protein is an autophagic substrate, and then favors aggresome formation.[41–43] SQSTM1 also accumulates in 16HBE14o- cells upon CFTR depletion as the result of disabled autophagy.[24] Here we demonstrate that in CFTR-depleted 16HBE14o- cells, Rab5 co-localized with SQSTM1 in intracellular aggregates (Figure 2c) and siRNA-mediated depletion of *SQSTM1*, together with that of CFTR, prevented both the sequestration of Rab5 in the insoluble protein fraction (Figure 2a) and the reduction of Rab5 and Rab7 protein levels (Figure 1b).

These results support the intimate connection between autophagy and endosomal trafficking.[31,32] They also indicate that CFTR depletion causes reduced Rab5 availability and likely perturbs endosomal function.

CFTR depletion impairs endosomal trafficking of surface receptors in bronchial epithelial cells. We examined the effects of CFTR depletion on the endocytic trafficking of two surface receptors: (i) the transferrin receptor (TfR), which recycles from the early/recycling endosomes to the PM[44] and (ii) the epidermal growth factor receptor (EGFR), which is sorted from the early endosomes towards degradative compartments (late endosomes (LEs)/lysosomes) following EGF-induced internalization.[45–47] As compared with scrambled siRNA-treated cells, CFTR-depleted 16HBE14o- cells exhibited reduced PM binding of Tf at 4 °C (Figure 3a), along with reduced cellular uptake of Tf (Figures 3b and c). This reduced uptake was due to impaired exposure of TfR to the cell surface rather than due to a defect in the internalization process *per se* (Figure 3d). Importantly, the recycling rates of internalized Tf were reduced by CFTR depletion (Figure 3e), in line with the observation that, after CFTR depletion, fluorescent-labelled Tf did not localize at $Rab11^+$ endosomes for up to 15 min after chase with unlabeled Tf, as this was the case in control conditions (Supplementary Figure S3A). Surface biotinylation and membrane fractionation confirmed the reduced exposure of TfR at the cell surface following CFTR depletion (Supplementary Figure S3B). The effects of CFTR depletion on TfR binding and recycling were abrogated by the enforced expression of HA-*BECN1* (Figure 3e), as well as by cystamine, unless 3-MA was added (Figure 3e; Supplementary Figures S3A and B).

To unravel whether the effects of CFTR depletion rely on the loss of CFTR function, we used the pharmacological CFTR inhibitor $CFTR_{inh\text{-}172}$. In spite of the fact that short-time CFTR-unrelated effects of $CFTR_{inh\text{-}172}$ have been described in CFTR lacking HeLa cells,[48] a long-term (24–48 h) treatment

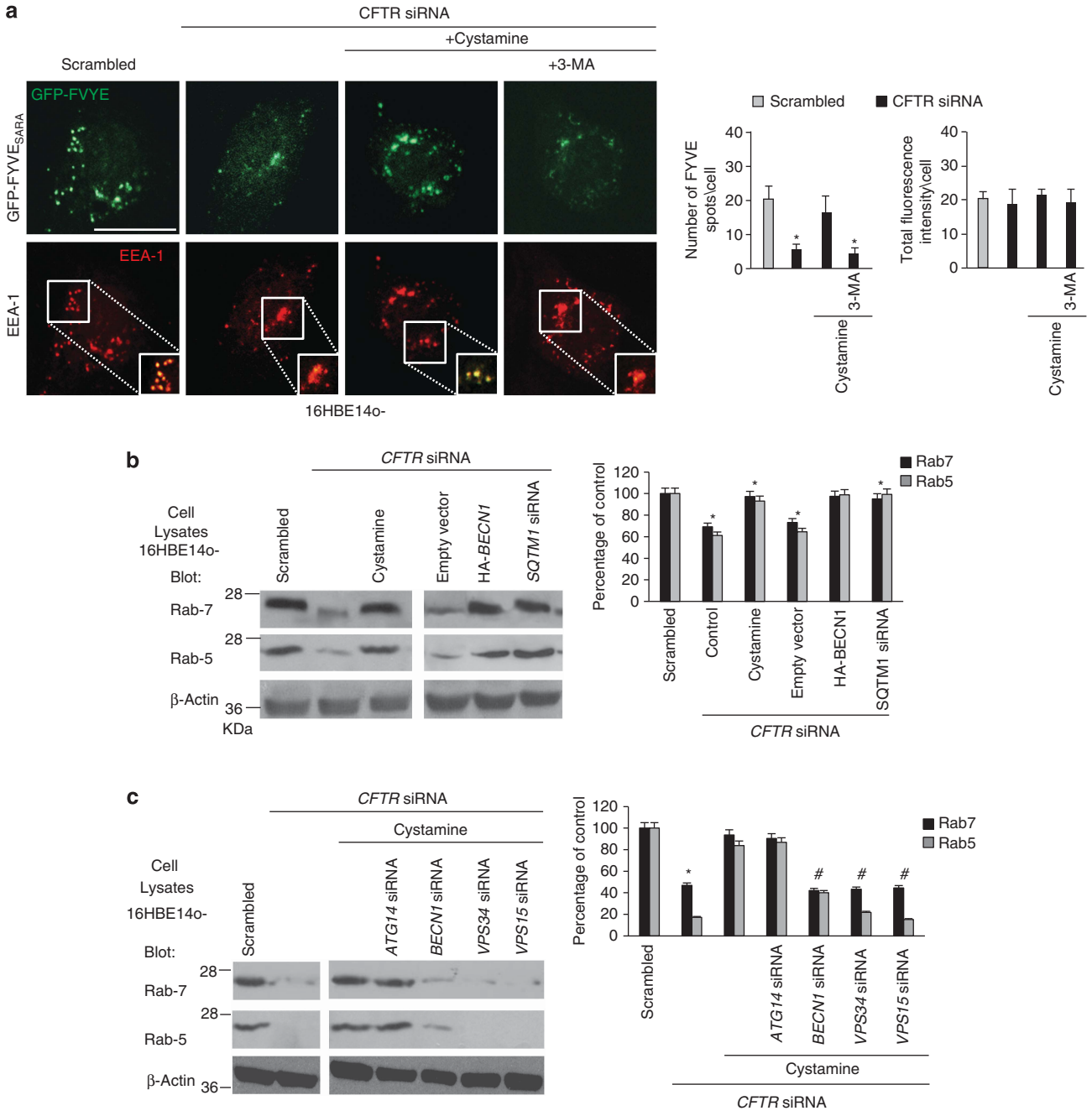

Figure 1 CFTR depletion reduces the availability of Rab5 and the recruitment of Rab5 effector EGFP-tagged-FYVE$_{SARA}$ to early endosomes. (**a**) Confocal microscopic images of 16HBE14o- cells transfected with a plasmid encoding EGFP-tagged-FYVE$_{SARA}$ and with CFTR-specific or scrambled siRNA (50 nM) in the presence or absence of cystamine (250 μM) with/without 3-MA (3 mM). Left, confocal microscopic images of EEA1 and EGFP-tagged-FYVE$_{SARA}$. Insets: boxed area show merged images of EGFP-tagged-FYVE$_{SARA}$ (green) and EEA1 (red). Scale bar, 10 μm. Right, number of FYVE$_{SARA}$ spots per cell were counted using AnalySIS software. Means ± S.D. ($n = 30$ cells per experiment; analysis of three independent experiments). *$P < 0.05$ compared with scrambled siRNA-treated cells. In this analysis, the total fluorescence intensity per cell was used to monitor EGFP-tagged-FYVE transfection efficiency and was calculated for each sample using Zeiss LSM 510 software (version 3.2). (**b**) Effects of CFTR depletion on Rab5 and Rab7 protein levels. Effects of cystamine (250 μM), HA-Beclin-1 overexpression or SQSTM1 siRNA (50 nM) in CFTR depleted 16HBE14o- cells. Left, Rab5 and Rab7 protein expression *versus* whole cell lysates. β-actin expression was measured as a loading control. Right, densitometric analysis of protein levels expressed as percentage of control. Mean ± S.D., *$P < 0.05$ compared with untreated cells, $^{\#}P < 0.01$ *versus* CFTR siRNA (analysis of variance (ANOVA)). (**c**) The cells were treated with or without CFTR siRNA (50 nM) in the presence or absence of cystamine (250 μM), after transfection with the indicated siRNAs (50 nM each). Left, expression of Rab5 and Rab7 in 16HBE14o- cells. Right, densitometric analysis of protein levels expressed as percentage of control. Mean ± S.D., *$P < 0.05$, compared with untreated cells, $^{\#}P < 0.01$ compared with cystamine-treated cells (ANOVA)

with CFTR$_{inh\text{-}172}$ led to CFTR-specific effects.[49,50] CFTR$_{inh\text{-}172}$ recapitulated the effects of CFTR depletion as it increased ROS-mediated TGM-2 SUMOylation and SQSTM1 levels only in 16HBE14o- but not in HeLa cells (Supplementary Figures S4A–C). In addition, CFTR$_{inh\text{-}172}$ was effective in favoring Rab5 sequestration within the insoluble

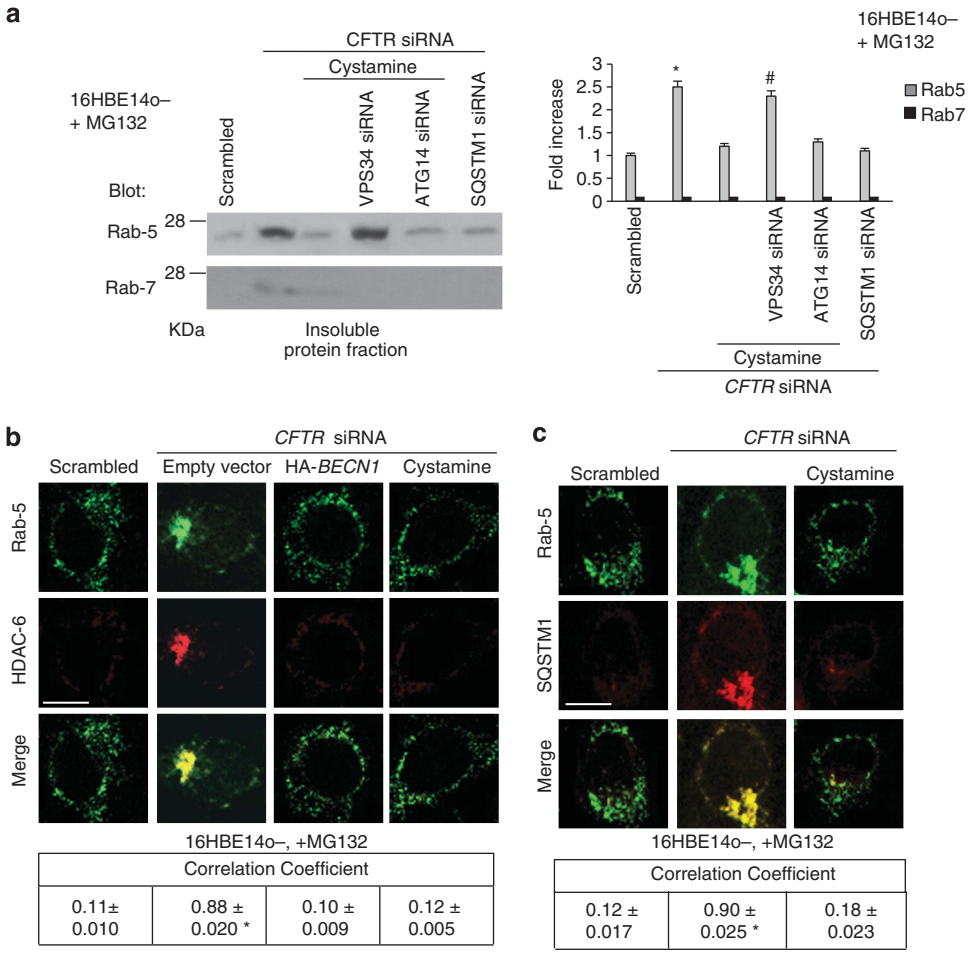

Figure 2 Effects of CFTR depletion on Rab5 distribution after proteasome inhibition in bronchial epithelial cells. (**a**–**c**) 16HBE14o- cells were treated with the proteasome inhibitor MG132 (50 μM). (**a**) The cells were treated with or without CFTR siRNA (50 nM) in the presence or absence of cystamine (250 μM) after transfection with the indicated siRNAs (50 nM each) or transfected with CFTR siRNA (50 nM) together with SQSTM1 siRNA (50 nM). Left, immunoblots of Rab5 and Rab7 in the detergent-insoluble fractions. Right, densitometric analysis of protein levels expressed as fold increase. Mean ± S.D., $^{*}P<0.05$ compared with scrambled siRNA-treated cells, $^{\#}P<0.01$ compared with cystamine-treated cells, (analysis of variance). (**b** and **c**) Effects of HA-Beclin-1 overexpression or cystamine (250 μM) in CFTR depleted 16HBE14o- cells. Cells were co-stained for Rab5 and HDAC6 (**b**) or with Rab5 and SQSTM1 (**c**). Upper, confocal microscopic images, bottom, quantitative measurement of co-localizations. Mean ± S.D. of five independent experiments ($n=50$ cells for each experiment). $^{*}P<0.05$ compared with scrambled siRNA-treated cells. Bar = 10 μm

protein fraction (Supplementary Figures S4D and E) as well as in impairing recycling of TfR in primary human bronchial epithelial cells (Figure 3f), thus recapitulating the effects of CFTR depletion from16HBE14o- cells.

We also investigated the effects of CFTR depletion on EGF-induced trafficking of the EGFR. In 16HBE14o- cells transfected with scrambled siRNAs, EGF (and its receptor) was efficiently degraded after 30 and 60 min of stimulation. By contrast, CFTR depletion delayed the EGFR degradation in 16HBE14o- cells, and EGFR was still retained up to 60 min following internalization (Figures 4a and b). HA-*BECN1* and cystamine neutralized these effects of CFTR depletion on EGFR degradation in a 3-MA-inhibitable fashion (Figures 4a and b).

Perturbed endosomal trafficking of TfR and EGFR was also observed in parental CFBE41o- cells, which lack a functional CFTR due to the homozygous ΔF508-CFTR mutation (Supplementary Figures S5A and B). Furthermore, Rab5 protein levels were significantly reduced in CFBE41o- cells, as Rab5 accumulated in the insoluble protein fraction even in the absence of incubation with the proteasomal inhibitor MG132 (Supplementary Figures S6A and B), in line with the observation that CF epithelial cells show SQSTM1 accumulation and proteasome overload as the result of the autophagy inhibition.[24]

Low Rab7 protein levels were detected in CFBE41o- cells, although Rab7 was not recovered from the detergent-insoluble protein fraction (Supplementary Figures S6A and B), suggesting impaired Rab5-Rab7 transition. Indeed, the Rab network also involves other components of the BECN1 interactome, such as UV-irradiation-resistance-associated gene (UVRAG) that interacts with the HOPS complex at the EEs, thus recruiting and activating Rab7 and favoring the Rab5 to Rab7 transition.[32,51] Decreased UVRAG impairs endosomal fusion and delays the endocytic trafficking and degradation of EGFR.[32,51] We found that in CFBE41o- cells UVRAG was sequestered within the detergent-insoluble protein fraction (Supplementary Figure

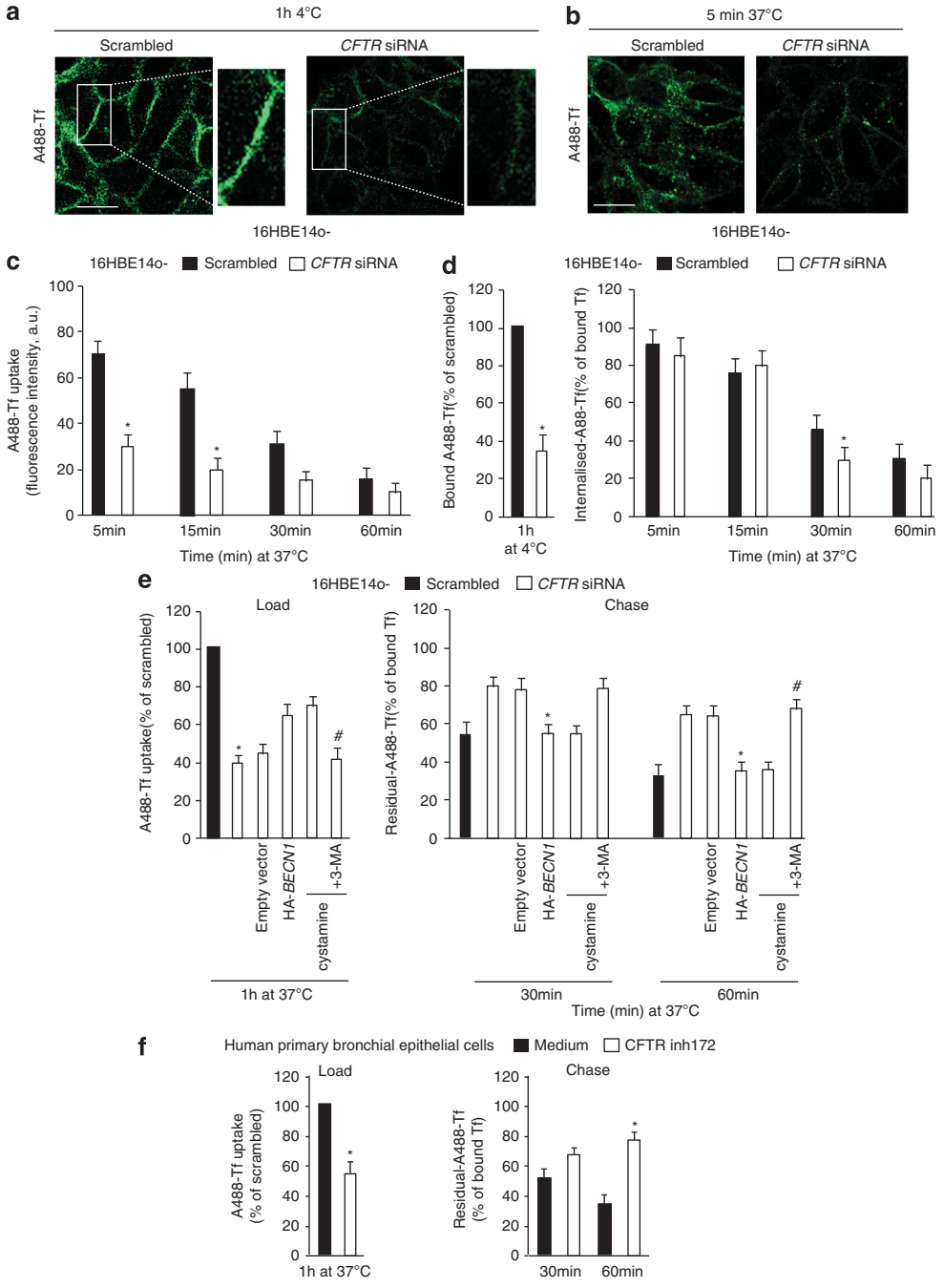

Figure 3 CFTR depletion impairs TfR recycling in bronchial epithelial cells. (**a**–**d**) 16HBE14o- cells were transfected with either 50 nM human CFTR siRNA or scrambled oligonucleotides. (**a**) The cells were exposed to Alexa-Fluor-488-Tf for 1 h at 4 °C (panel). Insets: enlargement of the boxed area, with images of Tf (green). (**b**) Then, the cells were warmed to 37 °C in complete medium for 5 min. Bar = 10 μm. (**c**) Quantification of cell-associated A488-Tf, evaluated as mean fluorescence intensities per cell at the indicated times, referred to the untreated samples and expressed as indicated (a.u., arbitrary units). Data are mean values ± S.D. ($n = 30$ cells; three independent experiments). *$P < 0.05$ compared with scrambled siRNA-treated cells, (analysis of variance (ANOVA)). (**d**) The PM exposure of Tf (Bound Al488-Tf) and its internalization (internalized Al488-Tf) were measured through binding at 4 °C and internalization at 37 °C for 5, 15, 30 and 60 min. The fluorescence intensities were quantified and expressed as percentages of bound Tf. Data are mean values ± S.D. ($n = 30$ cells; three independent experiments). *$P < 0.05$ compared with scrambled siRNA-treated cells (ANOVA). (**e**) 16HBE14o- cells were transfected with either 50 nM human CFTR siRNA or scrambled oligonucleotides in the presence of either HA-tagged BECN1 or the empty vector or cultured with cystamine (250 μM) followed by 3-MA (3 mM). For analysis of Tf recycling, the cells were loaded with Alexa-Fluor-488-Tf for 1 h at 37 °C (Load) and chased in complete medium for 30 and 60 min (Chase). The fluorescence intensities remaining in the cells after 30 and 60 min of chase were quantified and expressed as percentages of loaded Tf. Data are mean values ± S.D. ($n = 30$ cells; three independent experiments). *$P < 0.05$ compared with scrambled siRNA-treated cells, #$P < 0.01$ compared with cystamine treated cells (ANOVA). (**f**) Normal human primary bronchial epithelial cells were cultured in the presence of $CFTR_{inh172}$. For Tf recycling, the cells were loaded with Alexa-Fluor-488-Tf for 1 h at 37 °C (Load) and chased in complete medium for 30 and 60 min (Chase). The fluorescence intensities remaining in the cells after 30 and 60 min of chase were quantified and expressed as percentages of loaded Tf. Data are mean values ± S.D. ($n = 30$ cells; three independent experiments). *$P < 0.05$ compared with scrambled siRNA-treated cells (ANOVA)

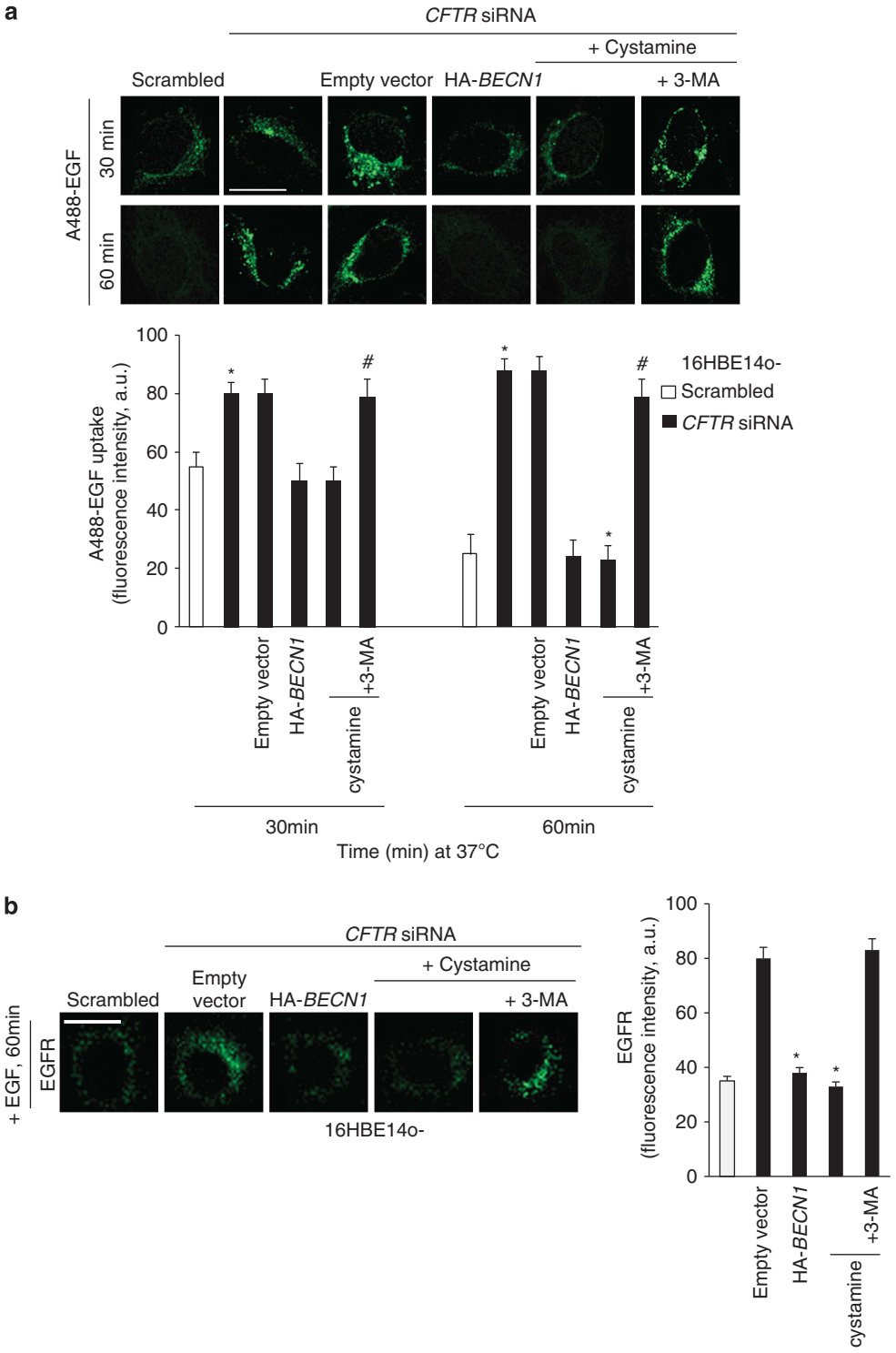

Figure 4 CFTR depletion delays EGFR endosomal trafficking in bronchial epithelial cells. (**a** and **b**) 16HBE14o- cells were transfected with either 50 nM human CFTR siRNA or scrambled oligonucleotides in the presence of either HA-BECN 1 or the empty vector or cultured with cystamine (250 μM) with/without 3-MA (3 mM). (**a**) Upper, the cells were serum starved for 12 h at 37 °C and then incubated for 1 h at 4 °C with 100 ng/ml EGF–AlexaFluor-488. The uptake of EGF and its movement along the endocytic pathway were followed by incubating the cells at 37 °C for the indicated times. Bar = 10 μm. Bottom, quantification of cell-associated A488-EGF, evaluated as mean fluorescence intensities per cell at the indicated times, and expressed as indicated (a.u., arbitrary units). Data are mean values ± S.D. ($n = 30$ cells; three independent experiments). $^{*}P < 0.05$ compared with scrambled siRNA-treated cells, $^{\#}P < 0.01$ compared with cystamine-treated cells (analysis of variance). (**b**) The cells were stimulated with EGF (100 ng/ml) for 60 min, fixed, permeabilized and labelled with antibodies against the EGFR. Bar = 10 μm. Bottom, quantification of cell-associated EGFR, evaluated as mean fluorescence intensities per cell and expressed as indicated (a.u.). Data are mean values ± S.D. ($n = 30$ cells; three independent experiments). $^{*}P < 0.05$ compared with scrambled siRNA-treated cells

S6C) and accumulated in HDAC6$^+$ aggregates (Supplementary Figure S6D). Cystamine effectively restored the soluble fraction of UVRAG protein (Supplementary Figure S6C).

Altogether, these results indicate that a functional CFTR is required for optimal endosomal trafficking of surface receptors in respiratory epithelial cells, thus regulating the abundance of the PM pool of surface proteins.

Functional inhibition of CFTR induces ubiquitination of CFTR protein and its interaction with SQSTM1 at the PM. We examined whether the function of CFTR would regulate the recycling of CFTR protein and hence its own PM stability. The abundance of CFTR at the PM is mainly determined by its recycling through the Rab11$^+$ endocytic pathway.[52,53] It has been reported that ubiquitylated CFTR becomes unstable at the PM and is diverted to lysosomal degradation.[54] Moreover, SQSTM1 can also function as a critical regulator of internalization, trafficking and sorting of ubiquitinylated surface proteins.[55,56] As SQSTM1 protein levels increase after functional CFTR depletion in 16HBE14o- cells (Supplementary Figure S4C), we wondered whether the functional CFTR inhibition might trigger the ubiquitination of CFTR at the PM, increase PM levels of SQSTM1 and hence stimulate CFTR/SQSTM1 interaction.

To this aim, we incubated 16HBE14o- cells with $CFTR_{inh\text{-}172}$ to analyze CFTR by means of anti-CFTR Abs. Addition of $CFTR_{inh\text{-}172}$ to 16HBE14o- cells increased the PM abundance of both SQSTM1 and the ubiquitin ligase carboxyl-terminus heat shock cognate 70 (Hsc70)–interacting protein (CHIP), a major player of PM protein quality control in CF[22] (Figure 5a). $CFTR_{inh\text{-}172}$ caused a dramatic increase in CFTR ubiquitination (which was barely detected in untreated 16HBE14o- cells) and enhanced the interaction between PM-resident CFTR and SQSTM1, as determined by co-immunoprecipitation (Figure 5b).

Moreover, after CFTR inhibition, both CFTR and SQSTM1 were detected within EEs, as revealed by subcellular fractionation followed by immunoblotting (Figure 5c). Accordingly, internalized CFTR co-localized with SQSTM1 at the epithelial surface as well as within enlarged vesicles in primary human bronchial epithelial cells treated with $CFTR_{inh\text{-}172}$ (Supplementary Figures S7A and B). Cystamine neutralized the effects of $CFTR_{inh\text{-}172}$ as it prevented PM ubiquitination of CFTR, SQSTM1 accumulation both at PM and in the endosomal compartment, as well as SQSTM1/CFTR interaction in bronchial epithelial cells (Figures 5a–c and Supplementary Figures S7A and B), unless 3-MA was added to the system (Supplementary Figure S7A). Next, we investigated whether the accumulation of SQSTM1 at EEs following CFTR inhibition could favor Rab5 sequestration. To this aim, we overexpressed either wild-type (wt)-SQSTM1 or a SQSTM1 mutant lacking the ubiquitin-binding domain (delta-UBA mutant) in 16HBE14o- cells in the presence or absence of $CFTR_{inh\text{-}172}$. The overexpression of wt-SQSTM1, but not that of delta-UBA SQSTM1, recapitulated the effects of CFTR inhibition in causing the redistribution of Rab5 into the detergent-insoluble protein fraction (Figures 5d and e). Moreover, the enforced expression of delta-UBA SQSTM1, but not that of wt-SQSTM1, abrogated these effects of CFTR inhibition (Figures 5d and e). These data indicate that the ubiquitin-binding activity of SQSTM1 is pivotal for inducing Rab5 sequestration within the detergent-insoluble protein fraction upon CFTR inhibition.

To determine whether functional inhibition of CFTR would lower its own recycling, we developed an assay in which 16HBE14o- cells were either left untreated or were pretreated with $CFTR_{inh\text{-}172}$ for 24 h, and cycloheximide (CHX) was added during the last 4 h of incubation to inhibit protein neosynthesis.[22,27] 16HBE14o- cells were then shifted to 4 °C for 1 h, followed by incubation at 37 °C to induce internalization of PM-resident endogenous CFTR. In contrast to untreated cells, $CFTR_{inh\text{-}172}$-treated cells manifested negligible CFTR localization in Rab11$^+$ endosomes 30 min after internalization (Figure 6a). The deranged recycling of CFTR following functional CFTR inhibition was reversed by cystamine unless BECN1 was depleted during cystamine treatment (Figure 6a). Moreover, in $CFTR_{inh\text{-}172}$-treated cells, CFTR was detected within LAMP1$^+$ vesicles as late as 90 min following internalization, unless SQSTM1 was depleted by siRNA (Figure 6b). Thus, functional inhibition of CFTR perturbs CFTR recycling as it diverts CFTR towards lysosomal degradation.

Altogether, these results indicate that the inhibition of CFTR function in bronchial epithelial cells enhances the function and abundance of SQSTM1 at the PM, thus favoring PM disposal of ubiquitylated CFTR and perturbing the endosomal routes that mediate CFTR recycling.

CFTR function controls CFTR protein stability at the PM of bronchial epithelial cells. The aforementioned data suggest that the function of CFTR may determine the stability of CFTR protein at the PM. To further explore this possibility, 16HBE14o- cells were incubated with $CFTR_{inh\text{-}172}$ for 24 h in the presence or absence of EUK-134 or cystamine with/without 3-MA, with CHX (100 μg/ml), which was added twice at 8 and 4 h before termination of the experiment.[27] CHX toxicity in the system was excluded by a 3-[4,5-dimethylthiazol-2-yl]-2,5 diphenyl tetrazolium bromide (MTT) cell viability assay (Supplementary Figures S8A and B). Then the abundance of CFTR at the PM was determined by cell-surface biotinylation, purification of biotinylated proteins and immunoblotting. $CFTR_{inh\text{-}172}$ reduced the overall abundance of PM-resident mature glycosylated CFTR (band C) by more than two-thirds (27% of remaining band C *versus* 91% in cells treated with CHX alone, considering 100% the value of untreated cells) (Figure 7a), and this effect was fully reversed by simultaneous addition of either cystamine or EUK-134 (88 and 85% of the remaining band C, respectively) unless 3-MA was added to the system or BECN1 was depleted by siRNAs (Figure 7a). Depletion of SQSTM1 also abrogated the capacity of $CFTR_{inh\text{-}172}$ to reduce the PM abundance of CFTR (Figure 7a). Finally, $CFTR_{inh\text{-}172}$ lowered the PM abundance of CFTR in a cystamine-inhibitable fashion, in primary human bronchial epithelial cells (Figure 7b), confirming the tight link between CFTR function and CFTR stability.

CFTR sufficiency is required for PM stability of the misfolded ΔF508-CFTR mutant. We previously reported that ΔF508-CFTR mutant protein, which has been rescued at the epithelial surface of ΔF508-CFTR homozygous epithelial

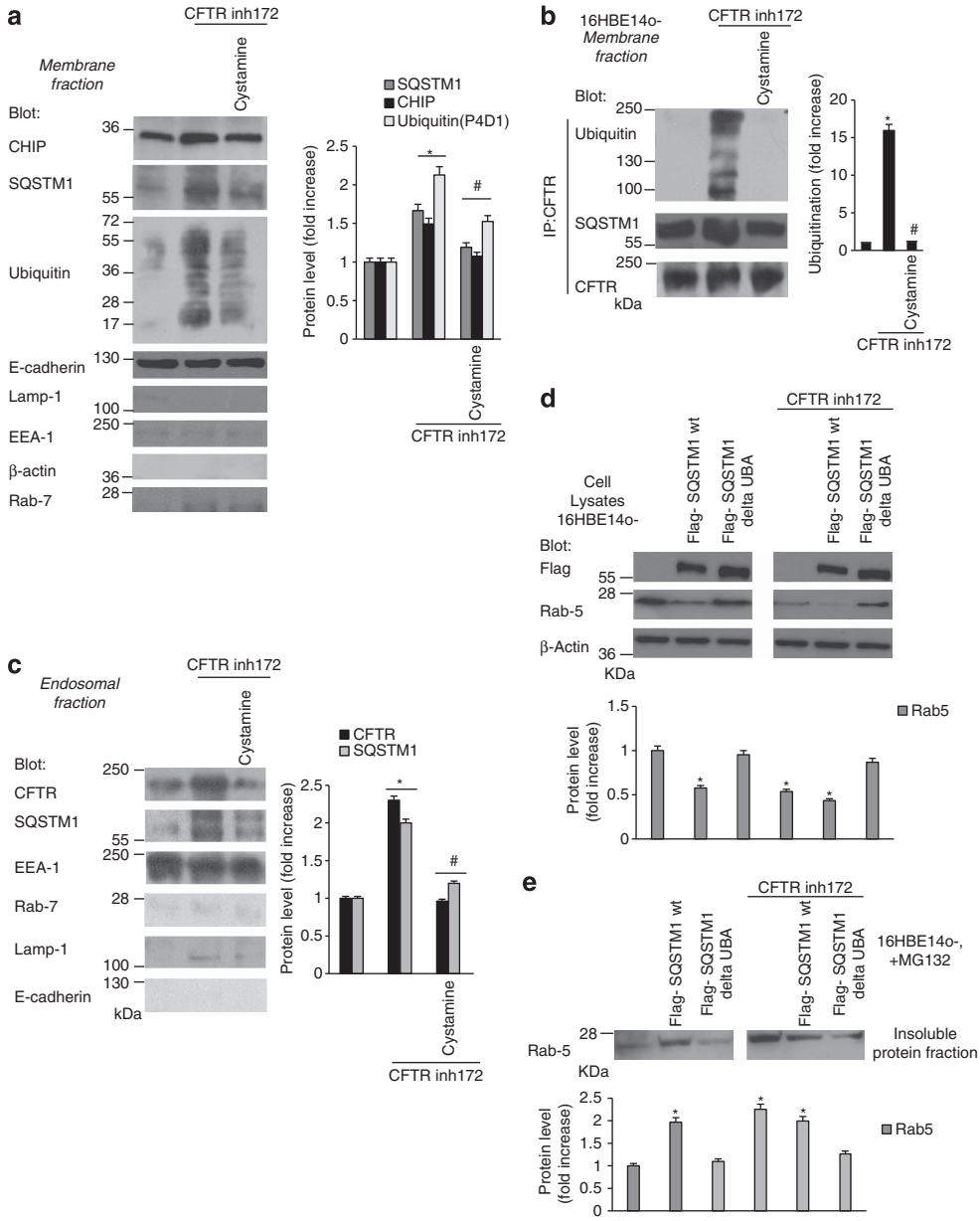

Figure 5 Functional inhibition of CFTR leads to ubiquitination of CFTR at the PM of bronchial epithelial cells together with interaction with SQSTM1. (**a** and **b**) 16HBE14o- cells were treated with $CFTR_{inh172}$ (20 μM) with/without cystamine (250 μM) in the presence of CHX during the last 8 h of incubation. The incubation for 4 h at 4 °C was used to block endocytosis. (**a**) Left, expression of CHIP, SQSTM1 and Ubiquitin (Ab, P4D1) from membrane fraction. E-Cadherin, LAMP1, EEA1, Rab7 and β-actin were used as control of the membrane cell-surface protein fractionation. Right, densitometric analysis of protein levels expressed as fold increase. Mean ± S.D., $^{*}P<0.05$ compared with untreated cells, $^{\#}P<0.01$ *versus* $CFTR_{inh172}$-treated (analysis of variance (ANOVA)). (**b**) Protein samples from the PM were immunoprecipitated with anti-CFTR (clone CF3) and immunoblotted with anti-CFTR (clone M3A7), anti-SQSTM1 or anti-Ubiquitin (P4D1) Abs. Immunoprecipitation was performed with 500 μg of protein samples. Right, densitometric analysis shows the abundance of ubiquitylated CFTR adducts normalized for the expression level of their band C and expressed as fold increase relative to that of untreated cells (means ± S.D. of three experiments). $^{*}P<0.05$ compared with untreated cells, $^{\#}P<0.01$ *versus* $CFTR_{inh172}$-treated (ANOVA). (**c**) 16HBE14o- cells were treated with $CFTR_{inh172}$ in the presence or absence of cystamine. After 15 min following internalization, early endosome fraction was purified by sucrose cushion and immunoblotted for the early endosome marker EEA1. The absence of the late endosome marker Rab7 or lysosome marker LAMP-1 or membrane marker E-Cadherin confirms fraction-specific labeling. Left, representative immunoblot analysis of CFTR (clone 3MA7) and SQSTM1 in EEA1 positive fraction. Right, densitometric analysis of protein levels expressed as fold increase. Mean ± S.D., $^{*}P<0.05$ compared with untreated cells, $^{\#}P<0.01$ *versus* $CFTR_{inh172}$-treated (ANOVA). (**d** and **e**) 16HBE14o- cells were transfected with Flag-SQSTM1-wt or Flag-SQSTM1-deltaUBA with or without $CFTR_{inh-172}$. (**d**) Upper, immunoblots of Rab5 in whole cell lysates. Flag was used as control of transfection. β-actin expression was measured as a loading control. Bottom, densitometric analysis of protein levels expressed as fold increase. Mean ± S.D., $^{*}P<0.05$ compared with untreated cells (ANOVA). (**e**) The cells were treated with the proteasome inhibitor MG132 (50 μM). Upper, immunoblots of Rab5 in the detergent-insoluble fractions. Bottom, densitometric analysis of protein levels expressed as fold increase. Mean ± S.D., $^{*}P<0.05$ compared with untreated cells (ANOVA)

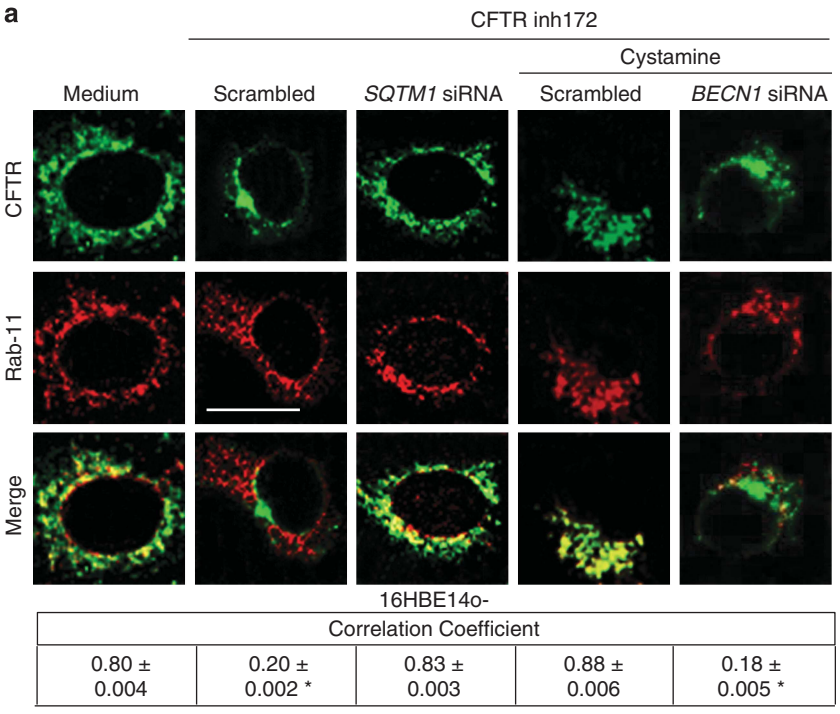

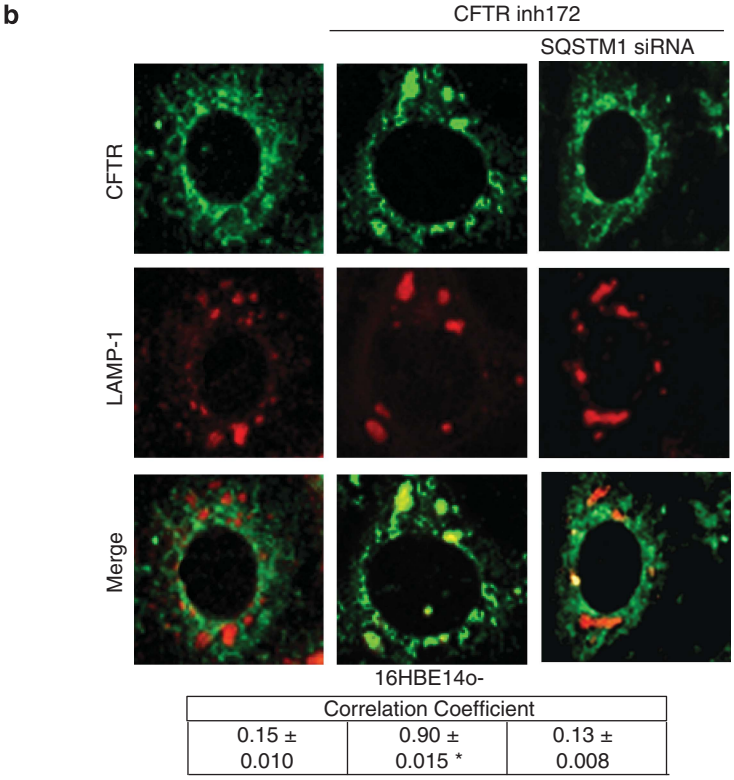

Figure 6 Functional inhibition of CFTR impairs CFTR recycling in bronchial epithelial cells. (**a**) 16HBE14o- cells were treated with $CFTR_{inh172}$ (20 μM) and/or 50 nM of scrambled or SQSTM1 siRNAs or cystamine in the presence or absence of BECN1 siRNAs. CHX (100 μg/ml) was added during the last 4 h. The cells were then shifted at 4 °C for 1 h and then at 37 °C up to 30 min to allow internalization. Upper, confocal microscopic images of CFTR co-stained with Rab11, 30 min after internalization. Bottom, quantitative measurement of co-localization. Mean ± S.D. of five independent experiments ($n = 50$ cells for each experiment). *$P < 0.05$ compared with untreated cells. Bar = 10 μm. (**b**) 16HBE14o- cells were treated with $CFTR_{inh172}$ (20 μM) and 50 nM of scrambled or SQSTM1 siRNAs. Upper, confocal microscopic images of CFTR (clone CF3) co-stained with LAMP1, 90 min after internalization. Bottom, quantitative measurement of co-localization. Mean ± S.D. of three independent experiments ($n = 50$ cells for each experiment). Representative of three different experiments. *$P < 0.05$ compared with untreated cells. Bar = 10 μm

cells by cystamine treatment, can reside at the PM well beyond cystamine washout. This suggests that ΔF508-CFTR might sustain its own PM stability. To address this issue, we tested whether a CFTR-sufficient context (i.e., untreated 16HBE14o- cells) could also generate a permissive environment for PM stability of the misfolded ΔF508-CFTR mutant.[22,27] We transfected 16HBE14o- cells with HA-tagged ΔF508-CFTR at 37 °C, an experimental condition that does not allow ΔF508-CFTR to traffic to the PM in cells that lack wt-CFTR expression.[3,4,6] Mature ΔF508-CFTR band C was detected in immunoblots of whole 16HBE14o- cell lysates with an anti-HA Ab (Supplementary Figure S9A). Twenty-four hours post transfection, the cells were cultured for 8 h in the presence of CHX (100 μg/ml, refreshed every 4 h) to inhibit protein neosynthesis, as described above. Immunoblotting of surface biotinylated proteins revealed that ΔF508-CFTR band C was stably expressed at the PM of 16HBE14o- even after 8 h following CXH treatment

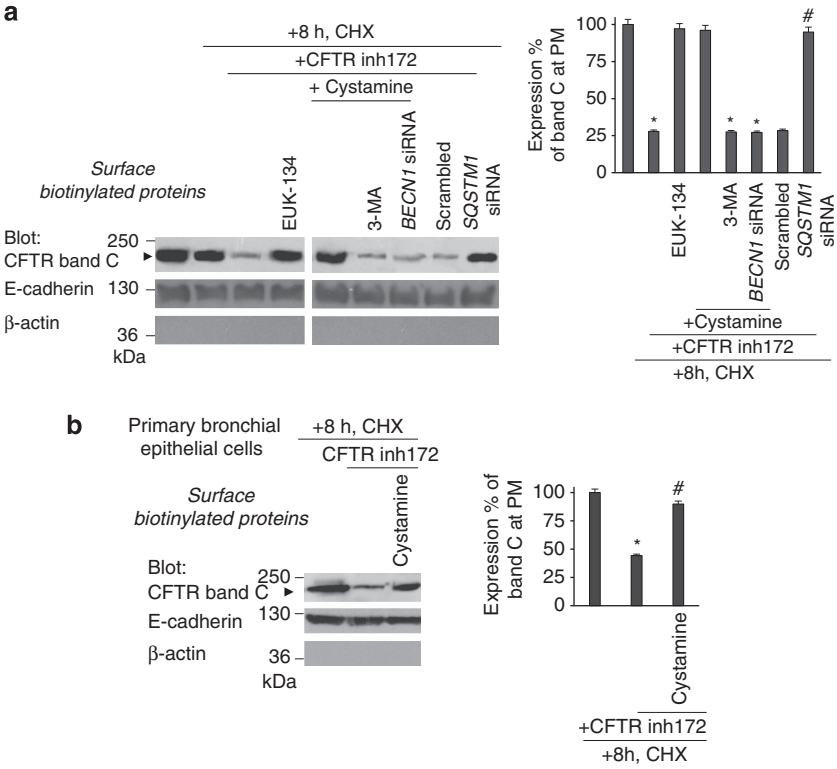

Figure 7 CFTR function controls CFTR protein stability at the PM of bronchial epithelial cells. (**a**) 16HBE14o- cells were incubated with/without $CFTR_{inh172}$ in the presence or absence of EUK-134 or cystamine with or without 3-MA or BECN1 siRNAs. $CFTR_{inh172}$-treated cells were alternatively transfected with SQSTM1 siRNAs. CHX (100 μg/ml) was added during the last 8 h of incubation. Left, Surface-biotinylated proteins from the PM and immunoblot with anti-CFTR Ab (clone M3A7). Right, densitometric measurement of the residual wt-CFTR band C at PM expressed as percentage of initial amount normalized to E-cadherin levels. Mean ± S.D. of triplicates of three different experiments; $^{*}P<0.05$, $^{\#}P<0.01$ compared with initial amount with CHX (analysis of variance (ANOVA)). (**b**) Normal human primary bronchial epithelial cells were treated with/without $CFTR_{inh172}$ in the presence or absence of cystamine. CHX (100 μg/ml) was added during the last 8 h of incubation. Left, surface-biotinylated proteins from the PM and immunoblot with anti-CFTR Abs (clone 3MA7). Right, densitometric measurement of the residual wt-CFTR band C at PM expressed as the percentage of initial amount normalized to E-cadherin levels. Mean ± S.D. of triplicates of three different experiments; $^{*}P<0.05$ compared with untreated cell, $^{\#}P<0.01$ *versus* $CFTR_{inh172}$-treated cells (ANOVA)

Figure 8 CFTR function is required for PM stability of ΔF508-CFTR in bronchial epithelial cells. (**a**) 16HBE14o- cells were transfected with HA-ΔF508-CFTR and then incubated with/without $CFTR_{inh\text{-}172}$ in the presence or absence of cystamine with/without 3-MA. CHX (100 μg/ml) was added during the last 8 h of incubation. Left, surface-biotinylated proteins from the PM were immunoblotted with anti-HA Ab. Right, densitometric analysis of the residual band C at PM expressed as the percentage of initial amount normalized to E-cadherin levels. Mean ± S.D. of triplicates of three different experiments; $^{*}P<0.05$ compared with untreated cells, $^{\#}P<0.01$ *versus* cystamine-treated cells (analysis of variance (ANOVA)). (**b**) 16HBE14o- were transfected with HA-ΔF508-CFTR and/or with scrambled or SQSTM1 siRNAs (50nM) and then incubated with $CFTR_{inh172}$ for 24 h. CHX was added during the last 8 h. Left, surface-biotinylated proteins from the PM of the transfected CFTR band C by anti-HA Abs. Right, densitometric analysis the residual band C at PM expressed as the percentage of initial amount normalized to E-cadherin levels. Mean ± S.D. of triplicates of three different experiments; $^{*}P<0.05$ compared with untreated cells, $^{\#}P<0.01$ *versus* scrambled treated cells incubated with $CFTR_{inh172}$ (ANOVA). (**c**) Schematic representation of the results. (1) CFTR inhibition leads to the sequestration of the BECN1 interactome as the result of TG2-mediated BECN1 crosslinking that reduces the availability of PtdIns3K (Vps34). This results in autophagy inhibition with accumulation of SQSTM1 (p62) leading to proteasome overload and accumulation of ubiquitin. The inhibition of CFTR function induces CFTR ubiquitination at the PM and favors the interaction between CFTR and p62. (2) The reduced PtdIns3K availability also decreases PtdIns3P at the early endosomes and reduces Rab5 protein levels, thus impairing endosomal function. The binding of p62 to ubiquitylated CFTR at the PM diverts CFTR recycling and targets CFTR to degradation. Moreover, p62 present at early endosomes favors Rab5 sequestration within insoluble protein aggregates and delays the progression of internalized CFTR though the degradative route, thus causing its local accumulation

(Figure 8a). However, pretreatment with $CFTR_{inh-172}$ strongly reduced the abundance of PM ΔF508-CFTR in this experimental setting, unless cystamine (but not cystamine combined with 3-MA) was added as well (Figure 8a). Direct depletion of *SQSTM1* by siRNAs mimicked the effects of cystamine (Figure 8b). Cystamine did not influence the PM abundance of ΔF508-CFTR rescued by low temperature in CFTR-lacking HeLa cells[54,57] (Supplementary Figure S10A), indicating that cystamine does not directly target ΔF508-CFTR and rather corrects the derangement of peripheral

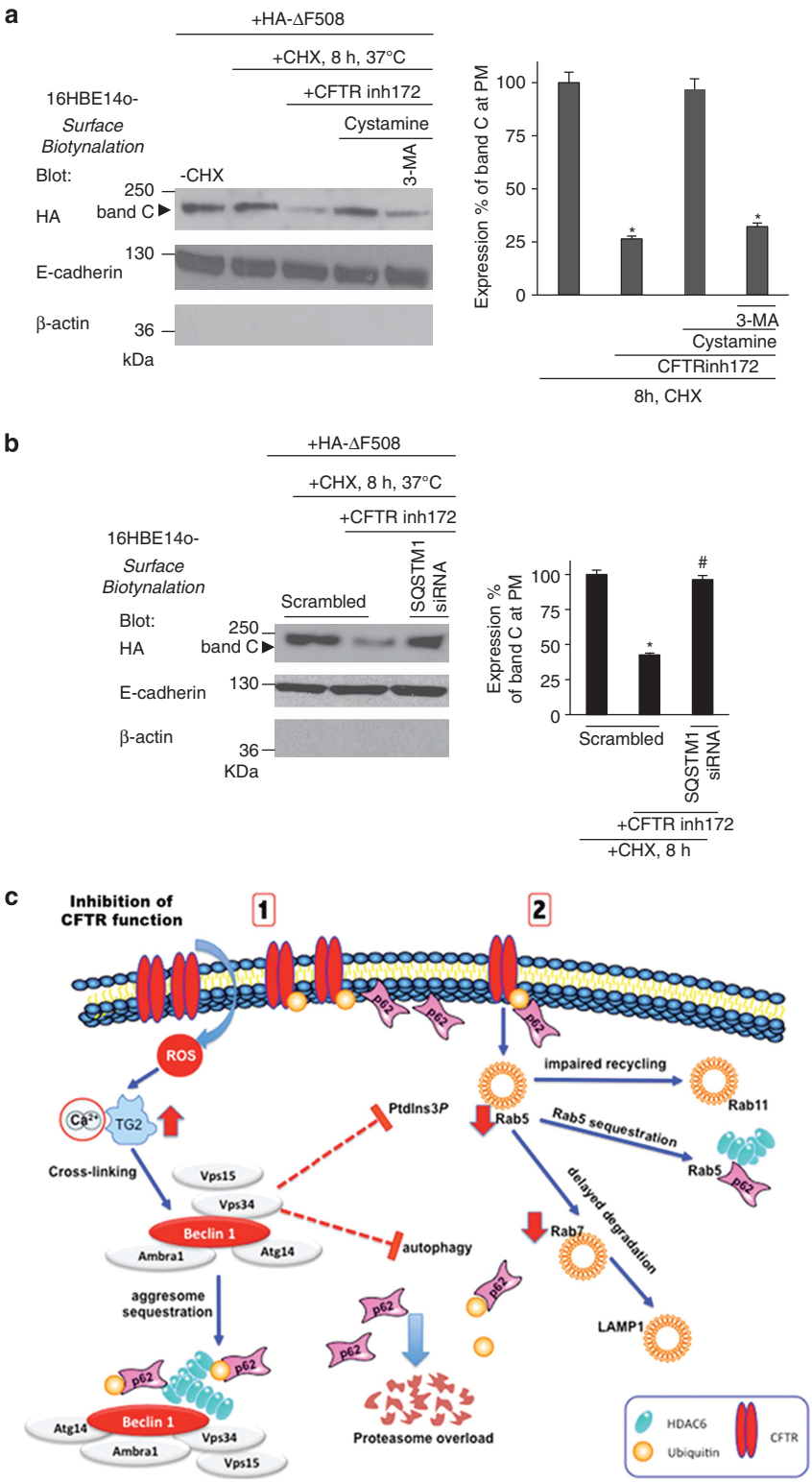

proteostasis resulting from CFTR inhibition in bronchial epithelial cells. These results indicate that a CFTR-sufficient context generates permissive conditions for ΔF508-CFTR mutant to reside at the PM of airway epithelial cells.

Discussion

The proteostasis network is a homeostatic system that responds to multiple perturbations, be they genetically determined or acquired due to environmental stress or aging. The accumulation of misfolded proteins secondary to destabilizing genetic mutations or the aging-related decline of proteostasis contributes to several human conformational diseases, including neurodegenerative disorders, type II diabetes and CF.[1–5]

This study indicates that CFTR is a key player of the proteostasis network of bronchial epithelial cells. Our results provide evidence in favor of the hypothesis that functional perturbation of CFTR affects endosomal trafficking of cell-surface proteins exemplified by TfR, EGFR and CFTR itself. This results from the functional sequestration of BECN1, which has two negative effects on intracellular trafficking related to CFTR.[24] First, CFTR depletion or inhibition reduces the local generation of PtdIns3*P*, which is pivotal in regulating endosomal fusion/maturation and trafficking,[28–32] by inducing functional sequestration of the BECN1-interactor hVps34. Second, CFTR depletion or inhibition and consequent BECN1 inactivation disables autophagy, thereby enhancing the abundance of SQSTM1 both at the EEs (thus favoring sequestration of Rab5 in the detergent-insoluble protein fraction and favoring its aggregation) and at the PM (thus targeting ubiquitinylated CFTR to degradation). SQSTM1 is an ubiquitin-binding protein that accumulates in conditions of defective autophagy, leading to proteasome overload and favoring aggresome formation.[42,43,58] Interestingly, direct depletion of SQSTM1 increases BECN1 protein levels (through reducing TGM-2 levels)[24] and recapitulates the effects of either genetic (by enforced expression) or pharmacological (by cystamine) rescue of BECN1 as it can restore ΔF508-CFTR at the epithelial surface and blunt lung inflammation in CF mice.[27] Here, we show that SQSTM1 depletion avoids the deleterious effects of the functional CFTR inhibition on PM abundance and recycling of CFTR protein. By contrast, enforced expression of SQSTM1, but not that of the delta-UBA SQSTM1 mutant, recapitulated the effects of CFTR inhibition on Rab5 sequestration. These results highlight SQSTM1 as a pivot of CFTR-mediated regulation of peripheral proteostasis (Figure 8c).

Altogether our data indicate that pharmacological or genetic inhibition of CFTR ignites the disposal of PM-resident CFTR. This may have important implications for CF, as it may initiate a CF-relevant vicious cycle in which the loss of CFTR function negatively impacts on the overall abundance of the protein within the PM, hence further reducing the function of CFTR. Such a scenario may explain how it is sufficient to temporarily interrupt this negative feed-forward loop, for instance, by transient treatment with cystamine, to obtain a long-lasting therapeutic effect that improves signs of lung inflammation in ΔF508-CFTR homozygous mice.[27] Indeed, re-establishing and sustaining a functional CFTR at the PM of bronchial epithelial cells generates permissive conditions for misfolded ΔF508-CFTR to traffic to and reside at the PM of bronchial epithelial cells.[27]

Conformational diseases are characterized by the premature degradation of unstable proteins or, on the contrary, their unwarranted and harmful accumulation in intra- or extracellular compartments. The common view is that such diseases are caused by mutations that directly affect the structure of the protein, resulting in abnormal proteostasis due to excessive or deficient proteolysis. To our knowledge, CFTR constitutes the first example of a disease-relevant protein that must be fully functional to avoid its premature degradation, hence unveiling an unexpected connection between protein function and proteostasis. The proteostasis network is probably unique to each cell type and tissue.[1,4,5] Indeed, many conformational diseases manifest as tissue-specific disorders, in spite of the fact that mutant proteins are expressed near-to-ubiquitously in many different tissues. Understanding whether other disease-relevant proteins might orchestrate proteostasis in their specific context could unveil new strategies for drug discovery in other conformational diseases.

Materials and Methods

Cell lines and treatments. Normal 16HBE14o- or CFTR-mutated CFBE41o- bronchial epithelial cells (kindly provided by D.C. Gruenert) were cultured with minimum essential medium (MEM) Earl's salt (200 mM L-Glutamine, 10% FBS and the appropriate amount of penicillin/streptomycin). Human, normal primary bronchial/tracheal epithelial cells or HeLa adenocarcinoma cell lines (LGC Promochem, Milan, Italy) were cultured as recommended by the American Type Culture Collection.

16HBE14o- cells were transfected with GFP-tagged FYVE domain of SARA (PtdIns3*P* probe, GFP-FYVE)[46] and then with CFTR-specific or scrambled siRNAs or incubated with $CFTR_{inh\text{-}172}$ for 24 h (20 μM, refreshed every 4 h, Calbiochem, Darmstadt, Germany) in the presence or absence of cystamine (250 μM, Sigma-Aldrich, St Louis, MO, USA) or EUK-134 (50μg/ml, Vinci-biochem, Florence, Italy) or HA-BECN1 overexpression[24] or scrambled or SQSTM1 siRNA. The cells were also treated with CFTR siRNA or $CFTR_{inh172}$ and incubated with cystamine in presence of BECN1, hVps34, hVps15 or ATG14 siRNAs or with cystamine with/without 3-MA (3 mM, Sigma-Aldrich). In another set of experiments, the cells were previously transfected with Flag-SQSTM1-wt or Flag-SQSTM1-ΔUBA(E396X) with or without $CFTR_{inh\text{-}172}$. The cells were also incubated with CHX (100 μg/ml, refreshed every 4 h, Sigma-Aldrich)[22,55] or with MG132 (50 μM for 6 h, Calbiochem) where indicated. CHX toxicity was excluded by a MTT cell viability assay, as previously described.[27] In other experiments, the cells were incubated at 4 °C for 1 h to block endocytosis and then shifted at 37 °C to allow CFTR internalization. In another set of experiments, the cells were previously transfected with HA-tagged-ΔF508-CFTR and then treated with $CFTR_{inh\text{-}172}$ with/without cystamine followed by 3-MA.

Human primary epithelial cells were incubated without/with $CFTR_{inh\text{-}172}$ in the presence or absence of cystamine.

CFBE41o- cells were transfected with HA-BECN1 or incubated with cystamine (250 μM, Sigma-Aldrich).[24,27]

HeLa cells were transfected with HA-tagged-ΔF508-CFTR and then incubated at 26 °C for 30 h with/without cystamine. CHX was added during the last 8 h.

Plasmids. The pcDNA3-HA-BECN 1 (gift from N. Mizushima), pcDNA3.1HA-ΔF508-CFTR (PRIMM), pCMV-Tag2bFLAG-SQSTM1 wt or pCMV-Tag2b-FLAG-SQSTM1-ΔUBA (E396X) (kind gift of Dr. Lynne J. Hocking, University of Aberdeen, UK)[59] and the GFP-tagged $FYVE_{SARA}$ domain (PtdIns3*P* probe) (kindly provided by S. Corvera) expression vectors were used for transfection experiments as described.[24] Empty vectors were used as control.

Transfection and RNA interference. Cells were transfected with 50 nM of CFTR (Invitrogen), SQSTM1, BECN1, hVps15, ATG14 (PRIMM, Milan, Italy), hVPS34 (Sigma-Aldrich) siRNA (Supplementary Table SI) or scrambled oligonucleotides by Lipo RnaiMax (Invitrogen, Carlsbad, CA, USA) according to the manufacturer's instructions or transfected with pcDNA3-HA-Beclin1, $GFP\text{-}FYVE_{SARA}$, pcDNA3-HA-ΔF508-CFTR, pCMV-Tag2bFLAG-SQSTM1wt or

pCMV-Tag2bFLAG-SQSTM1-ΔUBA(E396X) expression vectors, with the help of lipofectamine 2000 (Invitrogen), according to the manufacturer's instructions.

Immunoblot analysis, immunoprecipitation and CFTR ubiquitination. The whole or membrane fraction proteins were obtained from treated and untreated cells, harvested, lysed and the amounts of proteins were determined by a Bio-Rad protein assay (Bio-Rad, Hercules, CA, USA) to ensure equal protein loading before western blot analysis. Fifty micrograms of cell lysate were loaded in each lane. Immunoprecipitation and CFTR ubiquitination were performed with proteins of membrane fraction incubated at 4 °C for 8–12 h with CFTR antibody (clone CF3, Abcam, Cambridge, UK) followed by the addition of Protein A/G-agarose beads. After washing, the immunoprecipitated proteins were subjected to electrophoresis through 8% polyacrylamide gels, transferred to blotting membranes and analyzed. CFTR ubiquitination level was measured by densitometry and normalized to the CFTR level in the precipitate. Densitometric analysis was performed with Image J software (NIH, Bethesda, MD, USA); all data points were expressed as means ± S.D. of triplicates of three independent experiments.

Cell-surface biotinylation assay and membrane fractionation. Cell-surface proteins were biotinylated using sulfosuccinimidyl-6-(biotinamido) hexanoate (sulfo-NHS-LC-Biotin, 1 mg/ml in PBS, pH 8.2; Pierce, Rockford, IL, USA), as described.[27,60] Cells were homogenized with a Potter-Elvehjem pestle and centrifuged at 2300 × *g* for 15 min at 4 °C. Supernatants that contains the cytoplasmic and PM fractions were centrifuged 1 h at 16 000 × *g* at 4 °C; the pellet was the intact membrane and was solubilized in BUFFER A (20 mM Tris-HCl pH 7.4, 2 mM EDTA, 20 mM 2-ME, 1 × PMSF, 1 μg/ml inhibitor protease cocktail) + 1% Triton X-100 and centrifuged 1 h at 60 000 × *g* in the ultracentrifuge. The supernatants were collected as PM fraction. Equivalent amounts of protein (500 μg) were used for streptavidin-agarose pull-down (Pierce). Biotinylated proteins of PM fraction were immunoblotted against CFTR (clone M3A7) or TfR and E-cadherin or β–actin. For transferrin: cells were starved for 1 h at 37 °C in serum-free HEPES-buffered DMEM and then incubated for 1 h at 4 °C in the continuous presence of 5 μg/ml Tf-unconjugated (Invitrogen) HEPES-buffered DMEM. The cell were incubated at 37 °C for 15 min in growth medium and then processed for biotnylation assay. The densitometric analysis and percentage remaining was performed by Image J software and each data point is expressed as the mean ± S.D. of triplicate of three independent experiments.

Differential fractionation and separation of endosomes. The separation of EE and LE fractions was performed as described.[61] Briefly, cells were homogenized gently to limit damage to endosomes, and a post-nuclear supernatant (PNS) was prepared by centrifugation for 10 min at 1000 × *g*, and then the PNS was centrifuged at 20 000 × *g* for 20 min. The supernatant was collected, and the pellet was resuspended with 1 × homogenization buffer (250 mM sucrose, 1 mM Na_2EDTA, 10 mM HEPES). The PNS was adjusted to 40.6% sucrose, loaded at the bottom of an SW60 tube and then overlaid sequentially with 16% sucrose in D_2O, 10% sucrose in D_2O and finally with homogenization buffer. The gradient was centrifuged for 60 min at 60 000 × *g* using an SW60 rotor. EEs were then collected at the 16%/10% interface and LEs at the top of the 10% cushion.

Soluble and insoluble fractions. Cells were lysed in buffer containg 50 mM Tris- HCl pH 7.5, 150 mM NaCl, 0.5% Nonidet P40, 5 mM EDTA, 1 mM phenylmethylsulphonyl fluoride, 50 mM NaF, 10 μg/ml leupeptin and 10 μg/ml apoprotein supplemented with protease inhibitors (Sigma-Aldrich) in presence of 2% SDS and centrifuged at 16 000 × *g* at 4 °C for 20 min. After centrifugation, the soluble (supernatant) and insoluble (pellet) fraction were used in western blot analysis with anti-Rab5 antibody. The pellet insoluble in Nonidet P40 was dissolved five times in sample buffer, boiled at 95 °C for 5 min and resolved on a 10% polyacrylamide gel.[24]

Antibodies. The following primary antibodies were used for blot analysis: Ubiquitin (P4D1), 1 : 1000, CHIP, 1 : 500, hVps15\p150 (Nterm), 1 : 300, UVRAG, 1 : 500, Santa Cruz Biotechnology (Santa Cruz Inc, Santa Cruz, CA, USA); SQSTM1, 1 : 1000, hVps34, 1 : 500, ATG14L, 1 : 750, Flag 1:1500 (Sigma-Aldrich); CFTR clone M3A7, 1 : 500, EEA-1, 1 : 1000, Lamp-1, 1 : 1000, CFTR (CF3), 1 : 1000, Rab-5, 1 : 1000, Rab-7, 1 : 1000, BECN1, 1 : 1000, Abcam; E-Cadherin, 1 : 1000 and β-actin, 1 : 1000, Cell Signaling Technology (Cell Signaling Inc., Danvers, MA, USA); and TfR, 1 : 800, Invitrogen.

The following primary antibodies were used for microscopy techniques: mouse monoclonal antibodies against CFTR (CF3), 1 : 200, Abcam; SQSTM1(D3), 1 : 100, HDAC6 (D11), 1 : 100, UVRAG, 1 : 300, Santa Cruz Biotechnology; rabbit polyclonal antibodies against EEA-1, 1 : 400, Rab5, 1 : 400, LAMP-1, 1 : 400, Abcam; hVps-34, 1 : 500, SQSTM1, 1 : 400, Sigma-Aldrich; Rab11(D4F5), 1 : 400, Cell Signaling; CFTR(H-182), 1 : 100, EGFR (1005), 1 : 100, Santa Cruz Biotechnology. The Alexa-Fluor-488, Alexa-Fluor-546 secondary antibodies were obtained from Molecular Probes (Invitrogen).

Immunofluorescence and confocal imaging. The cells were fixed for 10 min with 4% paraformaldehyde (PFA, Sigma-Aldrich) in PBS, quenched with 50 mM NH_4Cl and permeabilized for 30 min in blocking buffer (0.1% (w/v) saponin, 0.5% (w/v) BSA in PBS/Ca/Mg). The cells were incubated for 2 h with the primary antibody, washed three times in PBS, incubated for 1 h with the secondary (Alexa-labelled) antibody, washed three times in PBS and were finally taken on Vectashield-mounted coverslips. The samples were examined under a Zeiss LSM 510 confocal laser-scanning microscope (Carl Zeiss MicroImaging, Thornwood, NY, USA) equipped with × 63 oil-immersion objective and image processing was done with Adobe Photoshop C2 (Adobe Sysytem Inc., San Jose, CA, USA). To perform quantitative image analysis, 10–15 randomly chosen fields that included 8–10 cells each were scanned, using the same setting parameters (i.e., pinhole, laser power, offset gain and detector amplification) below pixel saturation. The mean intensity per cell was determined using the histogram function in the Zeiss LSM 510 Software (version 3.2), and all of the pixel values above background levels were quantified. All of the experiments were repeated at least three times, and representative images are shown. Quantification of number of $FYVE_{SARA}$ spots per cell was performed using the AnalySIS software (Soft Imaging Systems GmbH, Muenster, Germany). To quantify the levels of co-localization, confocal serial sections were acquired from 8–10 cells per experimental condition, exported in TIFF format and processed as previously described.[62]

Tf uptake and recycling. For transferrin uptake, cells were starved for 1 h at 37 °C in serum-free HEPES-buffered DMEM and then incubated for 1 h at 4 °C in the continuous presence of 5 μg/ml Tf–Alexa-Fluor-488 (Molecular Probes) HEPES-buffered DMEM. The uptake of Tf and its movement along the endocytic pathway were followed by incubating the cells at 37 °C for 5, 10, 15, 30 and 60 min in growth medium. The cells were then treated with a mixture of 0.5 M NaCl and 0.5% acetic acid (this acid wash removes Tf that is non-specifically bound to the PM) for 30 s before being fixed and processed for immunofluorescence.

For transferrin recycling, cells were starved for 1 h at 37 °C, HEPES-buffered DMEM and then incubated for 20 min at 37 °C in the continuous presence of 5 μg/ml Tf–Alexa-Fluor-488 in serum-free, HEPES-buffered DMEM. After extensive washing with serum-free HEPES-buffered DMEM, the recycling of Tf was followed by incubating the cells at 37 °C in the presence of 50 μg/ml unlabelled Tf for 40 and 60 min in growth medium. The cells were then treated with a mixture of 0.5 M NaCl and 0.5% acetic acid for 30 s before being fixed and processed for immunofluorescence.

EGFR internalization and degradation. For EFGR internalization, the cells were serum starved for 12 h at 37 °C in serum-free HEPES-buffered DMEM to allow the EGFR to accumulate on the cell surface and then incubated for 1 h at 4 °C in the continuous presence of 100 ng/ml EGF–Alexa-Fluor-488 in serum-free HEPES-buffered DMEM. The uptake of EGF and its movement along the endocytic pathway were followed by incubating the cells at 37 °C for 5, 10,15, 30 and 60 min in growth medium. The cells were then treated with a mixture of 0.5 M NaCl and 0.5% acetic acid (this acid wash removes EGF that is non-specifically bound to the PM) for 30 s before being fixed and processed for immunofluorescence.

For EFGR degradation, the cells were stimulated by addition of EGF. At designated intervals after addition of EGF, cells were fixed, permeabilized and localization of the receptor was determined by immunofluorescence analysis using the antibody against total EGFR.

Fluorescence resonance energy transfer microscopy. Cells were immunostained with Alexa 546-anti-TG2 (Molecular Probes/Invitrogen)/Cy5-anti-SUMO-1 (Santa Cruz Biotechnology), as previously described.[24]

ROS detection. Cells were pulsed with 10 μM 5-(and-6)-chloromethyl-2′7′-dichlorodihydrofluorescein diacetate acetyl ester (Molecular Probes) and analyzed with Wallac 1420 multilabel Counter (Perkin Elmer, Zaventem, Belgium), as described.[24]

Iodide efflux. The analysis of the iodide efflux was performed by a iodide-sensitive fluorescent indicator, SPQ (Molecular Probes, Invitrogen), as previously described.[22,27,53,63] The rates were calculated using SigmaPlot Version 7.1 (Systat Software Inc., London, UK) for each mean fluorescence trace generated from the 50 cells examined per population per coverslip, as described.[27]

Statistical analysis. Data are reported as arithmetic mean ± S.D. Data distribution was analyzed for normality and statistical analysis performed using the one-way ANOVA. Significant differences are indicated in the figures. All data were obtained from independent measurements. Data were analyzed using SPSS 13 software (SPSS, Milan, Italy). Statistical significance was defined as *P*-value of <0.05.

Conflict of Interest

The authors declare no conflict of interest.

Acknowledgements. This work was supported by the European Institute for Research in Cystic Fibrosis and Italian Cystic Fibrosis Association (LM), the Programma di Ricerca Scientifica di Rilevante Interesse Nazionale (2008RMJB3A_004, 2008) of the ministero dell'Istruzione, dell'Università e della Ricerca (LM, VR), RO1 HL093004 (EMB), Telethon Grant No. GGP12128 (LM, EMB, VR, MCM), Ligue Nationale contre le Cancer (Equipe labellisée) (GK), AXA Chair for Longevity Research, Agence Nationale pour la Recherche (ANR) (GK), European Commission (ArtForce) (GK), Fondation pour la Recherche Médicale (FRM), Institut National du Cancer (INCa), Cancéropôle Ile-de-France (GK), Fondation Bettencourt-Schueller and the LabEx Onco-Immunology (GK). We thank Noboru Mizushima (The Tokyo Metropolitan Institute of Medical Sciences, Tokyo, Japan) for the gift of the pcDNA3-HA-Beclin1 expression vectors, Dieter C. Gruenert (University of California, San Francisco, CA, USA) for the gift of CFBE41o- cell lines, S. Corvera (University of Massachusetts Medical School, Worcester, MA, USA) for the gift of the GFP-FYVE$_{SARA}$. We thank Alessandro Luciani (European Institute for Research in Cystic Fibrosis, Milan) for technical assistance in confocal microscopy.

Author contributions

VRV co-designed the research concept, performed surface biotinylation and membrane fractionation, immunoblot and immunoprecipitation experiments, cell cultures and transfections and analyzed data. SE performed immunoblot and immunoprecipitation experiments, confocal microscopy, cell cultures and transfections and analyzed data. EMB provided the scientific knowledge, contributed to the discussion, interpretation and analysis of the data. MV provided the scientific knowledge, supervised confocal microscopic studies and contributed to the discussion, interpretation and analysis of the data. SC provided the SQSTM1 plasmids, provided the scientific knowledge on SQSTM1 mutants and contributed to the analysis of the data. ADM and AL provided the scientific knowledge and contributed to the discussion, interpretation and analysis of the data. SG, MPM and RC contributed to the discussion of data. VR, MCM and GK co-designed the research concept, co-supervised the project, provided the scientific knowledge and contributed to the discussion, interpretation and analysis of the data. LM designed the research concept, planned the overall experimental design and supervised the study. LM, VR and GK wrote the paper.

1. Powers ET, Morimoto RI, Dillin A, Kelly JW, Balch WE. Biological and chemical approaches to diseases of proteostasis deficiency. *Annu Rev Biochem* 2009; **78**: 959–991.
2. Hutt DM, Powers ET, Balch WE. The proteostasis boundary in misfolding diseases of membrane traffic. *FEBS Lett* 2009; **583**: 2639–2646.
3. Roth DM, Balch WE. Modeling general proteostasis: proteome balance in health and disease. *Curr Opin Cell Biol* 2011; **23**: 126–134.
4. Gidalevitz T, Kikis EA, Morimoto RI. A cellular perspective on conformational disease: the role of genetic background and proteostasis networks. *Curr Opin Struct Biol* 2010; **20**: 23–32.
5. Balch WE, Morimoto RI, Dillin A, Kelly JW. Adapting proteostasis for disease intervention. *Science* 2008; **319**: 916–919.
6. Balch WE, Roth DM, Hutt DM. Emergent properties of proteostasis in managing cystic fibrosis. *Cold Spring Harb Perspect Biol* 2011; **3**: a004499.
7. Okiyoneda T, Apaja PM, Lukacs GL. Protein quality control at the plasma membrane. *Curr Opin Cell Biol* 2011; **23**: 483–491.
8. Amaral MD. Targeting CFTR: how to treat cystic fibrosis by CFTR-repairing therapies. *Curr Drug Targets* 2011; **12**: 683–693.
9. O'Sullivan BP, Freedman SD. Cystic fibrosis. *Lancet* 2009; **373**: 1891–1904.
10. Rowe SM, Miller S, Sorscher EJ. Cystic fibrosis. *N Engl J Med* 2005; **352**: 1992–2001.
11. Accurso FJ. Update in cystic fibrosis 2005. *Am J Respir Crit Care Med* 2006; **173**: 944–947.
12. Park HW, Nam JH, Kim JY, Namkung W, Yoon JS, Lee JS *et al.* Dynamic regulation of CFTR bicarbonate permeability by [Cl-]i and its role in pancreatic bicarbonate secretion. *Gastroenterology* 2010; **139**: 620–631.
13. Welsh MJ, Smith AE. Molecular mechanisms of CFTR chloride channel dysfunction in cystic fibrosis. *Cell* 1993; **73**: 1251–1254.
14. Bobadilla JL, Macek M, Fine JP, Farrell PM. Cystic fibrosis: a worldwide analysis of CFTR mutations–correlation with incidence data and application to screening. *Hum Mutat* 2002; **19**: 575–606.
15. Kartner N, Augustinas O, Jensen TJ, Naismith AL, Riordan JR. Mislocalization of delta F508 CFTR in cystic fibrosis sweat gland. *Nat Genet* 1992; **1**: 321–327.
16. Okiyoneda T, Lukacs GL. Cell surface dynamics of CFTR: the ins and outs. *Biochim Biophys Acta* 2007; **1773**: 476–479.
17. Pedemonte N. Small-molecule correctors of defective [Delta]F508-CFTR cellular processing identified by high-throughput screening. *J Clin Invest* 2005; **115**: 2564–2571.
18. Galietta LJ, Springsteel MF, Eda M, Niedzinski EJ, By K, Haddadin MJ *et al.* Novel CFTR chloride channel activators identified by screening of combinatorial libraries based on flavone and benzoquinolizinium lead compounds. *J Biol Chem* 2001; **276**: 19723–19728.
19. Van Goor F, Straley KS, Cao D, González J, Hadida S, Hazlewood A *et al.* Rescue of DeltaF508-CFTR trafficking and gating in human cystic fibrosis airway primary cultures by small molecules. *Am J Physiol Lung Cell Mol Physiol* 2006; **290**: L1117–L1130.
20. Van Goor F, Hadida S, Grootenhuis PD, Burton B, Stack JH, Straley KS *et al.* Correction of the F508del-CFTR protein processing defect *in vitro* by the investigational drug VX-809. *Proc Natl Acad Sci USA* 2011; **108**: 18843–18848.
21. Denning GM, Anderson MP, Amara JF, Marshall J, Smith AE, Welsh MJ. Processing of mutant cystic fibrosis transmembrane conductance regulator is temperature-sensitive. *Nature* 1992; **358**: 761–764.
22. Okiyoneda T, Barriere H, Bagdany M, Rabeh WM, Du K, Hohfeld J *et al.* Peripheral protein quality control removes unfolded CFTR from the plasma membrane. *Science* 2010; **329**: 805–810.
23. Lukacs GL, Verkman AS. CFTR: folding, misfolding and correcting the DeltaF508 conformational defect. *Trends Mol Med* 2012; **18**: 81–91.
24. Luciani A, Villella VR, Esposito S, Brunetti-Pierri N, Medina D, Settembre C *et al.* Defective CFTR induces aggresome formation and lung inflammation in cystic fibrosis through ROS-mediated autophagy inhibition. *Nat Cell Biol* 2010; **12**: 863–875.
25. Luciani A. SUMOylation of tissue transglutaminase as link between oxidative stress and inflammation. *J Immunol* 2009; **183**: 2775–2784.
26. Maiuri L, Luciani A, Giardino I, Raia V, Villella VR, D'Apolito M *et al.* Tissue transglutaminase activation modulates inflammation in cystic fibrosis via PPAR gamma down-regulation. *J Immunol* 2008; **180**: 7697–7705.
27. Luciani A, Villella VR, Esposito S, Gavina M, Russo I, Silano M *et al.* Targeting autophagy as a novel strategy for facilitating the therapeutic action of potentiators on ΔF508 cystic fibrosis transmembrane conductance regulator. *Autophagy* 2012; **8**: 1657–1672.
28. Poteryaev D, Datta S, Ackema K, Zerial M, Spang A. Identification of the switch in early-to-late endosome transition. *Cell* 2010; **141**: 497–508.
29. Cabrera M, Ungermann C. Guiding endosomal maturation. *Cell* 2010; **141**: 404–406.
30. Rink J, Ghigo E, Kalaidzidis Y, Zerial M. Rab conversion as a mechanism of progression from early to late endosomes. *Cell* 2005; **122**: 735–749.
31. Ravikumar B, Imarisio S, Sarkar S, O'Kane CJ, Rubinsztein DC. Rab5 modulates aggregation and toxicity of mutant huntingtin through macroautophagy in cell and fly models of Huntington disease. *J Cell Sci* 2008; **121**: 1649–1660.
32. Thoresen SB, Pedersen NM, Liestol K, Stenmark H. A phosphatidylinositol 3-kinase class III sub-complex containing VPS15, VPS34, Beclin 1, UVRAG and BIF-1 regulates cytokinesis and degradative endocytic traffic. *Exp Cell Res* 2010; **316**: 3368–3378.
33. Christoforidis S, Miaczynska M, Ashman K, Wilm M, Zhao L, Yip SC *et al.* Phosphatidylinositol-3-OH kinases are Rab5 effectors. *Nat Cell Biol* 1999; **1**: 249–252.
34. Simonsen A, Gaullier JM, D'Arrigo A, Stenmark H. The Rab5 effector EEA1 interacts directly with syntaxin-6. *J Biol Chem* 1999; **274**: 28857–28860.
35. Hayakawa A, Hayes SJ, Lawe DC, Sudharshan E, Tuft R, Fogarty K *et al.* Structural basis for endosomal targeting by FYVE domains. *J Biol Chem* 2004; **279**: 5958–5966.
36. Gillooly DJ, Morrow IC, Lindsay M, Gould R, Bryant NJ, Gaullier JM *et al.* Localization of phosphatidylinositol 3-phosphate in yeast and mammalian cells. *EMBO J* 2000; **19**: 4577–4588.
37. Raiborg C, Bremnes B, Mehlum A, Gillooly DJ, D'Arrigo A, Stang E *et al.* FYVE and coiled-coil domains determine the specific localisation of Hrs to early endosomes. *J Cell Sci* 2001; **114**: 2255–2263.
38. Hu Y, Chuang JZ, Xu K, McGraw TG, Sung CH. SARA, a FYVE domain protein, affects Rab5-mediated endocytosis. *J Cell Sci* 2002; **115**: 4755–4763.
39. Sinha S, Levine B. The autophagy effector Beclin 1: a novel BH3-only protein. *Oncogene* 2008; **27**: S137–S148.
40. Kroemer G, Marino G, Levine B. Autophagy and the integrated stress response. *Mol Cell* 2010; **40**: 280–293.
41. Kirkin V, McEwan DG, Novak I, Dikic I. A role for ubiquitin in selective autophagy. *Mol Cell* 2009; **34**: 259–269.

42. Moscat J, Diaz-Meco MT. p62 at the crossroads of autophagy, apoptosis, and cancer. *Cell* 2009; **137**: 1001–1004.
43. Korolchuk VI, Mansilla A, Menzies FM, Rubinsztein DC. Autophagy inhibition compromises degradation of ubiquitin-proteasome pathway substrates. *Mol Cell* 2009; **33**: 517–527.
44. Maxfield FR, McGraw TE. Endocytic recycling. *Nat Rev Mol Cell Biol* 2004; **5**: 121–132.
45. Scita G, Di Fiore PP. The endocytic matrix. *Nature* 2010; **463**: 464–473.
46. Vicinanza M, Di Campli A, Polishchuk E, Santoro M, Di Tullio G, Godi A *et al.* OCRL controls trafficking through early endosomes via PtdIns4,5P(2)-dependent regulation of endosomal actin. *EMBO J* 2011; **30**: 4970–4985.
47. Daniele T, Di Tullio G, Santoro M, Turacchio G, De Matteis MA. ARAP1 regulates EGF receptor trafficking and signalling. *Traffic* 2008; **9**: 2221–2235.
48. Kelly M, Trudel S, Brouillard F, Bouillaud F, Colas J, Nguyen-Khoa T *et al.* Cystic fibrosis transmembrane regulator inhibitors CFTR(inh)-172 and GlyH-101 target mitochondrial functions, independently of chloride channel inhibition. *J Pharmacol Exp Ther* 2010; **333**: 60–69.
49. Ma T, Thiagarajah JR, Yang H, Sonawane ND, Folli C, Galietta LJ *et al.* Thiazolidinone CFTR inhibitor identified by high-throughput screening blocks cholera toxin-induced intestinal fluid secretion. *J Clin Invest* 2002; **110**: 1651–1658.
50. Baudouin-Legros M, Colas J, Moriceau S, Kelly M, Planelles G, Edelman A *et al.* Long-term CFTR inhibition modulates 15d-prostaglandin J2 in human pulmonary cells. *Int J Biochem Cell Biol* 2012; **44**: 1009–1018.
51. Liang C. Beclin1-binding UVRAG targets the class C Vps complex to coordinate autophagosome maturation and endocytic trafficking. *Nat Cell Biol* 2008; **10**: 776–787.
52. Cholon DM, O'Neal WK, Randell SH, Riordan JR, Gentzsch M. Modulation of endocytic trafficking and apical stability of CFTR in primary human airway epithelial cultures. *Am J Physiol Lung Cell Mol Physiol* 2010; **298**: L304–L314.
53. Silvis MR, Bertrand CA, Ameen N, Golin-Bisello F, Butterworth MB, Frizzell RA *et al.* Rab11b regulates the apical recycling of the cystic fibrosis transmembrane conductance regulator in polarized intestinal epithelial cells. *Mol Biol Cell* 2009; **20**: 2337–2350.
54. Sharma M, Pampinella F, Nemes C, Benharouga M, So J, Du K *et al.* Misfolding diverts CFTR from recycling to degradation: quality control at early endosomes. *J Cell Biol* 2004; **164**: 923–933.
55. Samuels IS, Seibenhener ML, Neidigh KB, Wooten MW. Nerve growth factor stimulates the interaction of ZIP/p62 with atypical protein kinase C and targets endosomal localization: evidence for regulation of nerve growth factor-induced differentiation. *J Cell Biochem* 2001; **82**: 452–466.
56. Geetha T, Wooten MW. TrkA receptor endolysosomal degradation is both ubiquitin and proteasome dependent. *Traffic* 2008; **9**: 1146–1156.
57. Delaney SJ, Rich DP, Thomson SA, Hargrave MR, Lovelock PK, Welsh MJ *et al.* Cystic fibrosis transmembrane conductance regulator splice variants are not conserved and fail to produce chloride channels. *Nat Genet* 1993; **4**: 426–431.
58. Korolchuk VI, Menzies FM, Rubinsztein DC. Mechanisms of cross-talk between the ubiquitin-proteasome and autophagy-lysosome systems. *FEBS Lett* 2010; **584**: 1393–1398.
59. Hocking LJ, Mellis DJ, McCabe PS, Helfrich MH, Rogers MJ. Functional interaction between sequestosome-1/p62 and autophagy-linked FYVE-containing protein WDFY3 in human osteoclasts. *Biochem Biophys Res Commun* 2010; **402**: 543–548.
60. Caohuy H, Jozwik C, Pollard HB. Rescue of [Delta]F508-CFTR by the SGK1/Nedd4-2 signaling pathway. *J Biol Chem* 2009; **284**: 25241–25253.
61. Aniento F, Emans N, Griffiths G, Gruenberg J. Cytoplasmic dynein-dependent vesicular transport from early to late endosomes. *J Cell Biol* 1993; **123**: 1373–1387.
62. Maiuri L, Luciani A, Villella VR, Vasaturo A, Giardino I, Pettoello-Mantovani M *et al.* Lysosomal accumulation of gliadin p31-43 peptide induces oxidative stress and tissue transglutaminase-mediated PPAR gamma downregulation in intestinal epithelial cells and coeliac mucosa. *Gut* 2010; **59**: 311–319.
63. Verkman AS, Galietta LJ. Chloride channels as drug targets. *Nat Rev Drug Discov* 2009 **8**: 153–171.

Supplementary Information accompanies this paper on Cell Death and Differentiation website (http://www.nature.com/cdd)